Industrial Crops & Products 227 (2025) 120805

Contents lists available at ScienceDirect

Industrial Crops & Products

journal homepage: www.elsevier.com/locate/indcrop

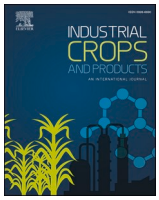

Molecular dynamics interpretation of citric acid-water assisting mechanism in deep eutectic solvent to destruct agricultural residue and improve enzymatic hydrolyzability of cellulose

Shaonuo Zhou [a,b,c], Xiaolei Zhang [d], Yong Xu [a,b,c,*]

[a] Jiangsu Co-Innovation Center of Efficient Processing and Utilization of Forest Resources, College of Chemical Engineering, Nanjing Forestry University, Nanjing 210037, PR China
[b] Jiangsu Province Key Laboratory of Green Biomass-based Fuels and Chemicals, Nanjing 210037, PR China
[c] Key Laboratory of Forestry Genetics & Biotechnology (Nanjing Forestry University), Ministry of Education, Nanjing 210037, PR China
[d] Department of Chemical and Process Engineering, University of Strathclyde, Glasgow G1 1XJ, United Kingdom

ARTICLE INFO

Keywords:
Biorefinery
Biomass pretreatment
DES
Enzyme hydrolysis of cellulose
Molecular dynamics simulation

ABSTRACT

Efficient pretreatment is so far the bottleneck in lignocellullosic biorefinery. The deep eutectic solvent (DES) technologies presents promising potentials except for some practical tasks that prohibits its designs and applications. By introducing citric acid (CA) and water into choline chloride (ChCl)-glycerol (GL) system, a ternary deep eutectic solvent (TDES) composed with 1:1:1 ChCl:CA:GL (n/n) exhibited more outstanding pretreatment efficiency for sugarcane bagasse (SB), a representative agricultural residue, in respect to enzyme hydrolysis of cellulose than traditional binary DES pretreatment. After pretreated with TDES containing 20 % water for 60 min in 100 ℃, the SB residue released 96.4 % of glucose by 20 FPIU/g cellulose of enzyme hydrolysis. To understand the chemical mechanism of this phenomenon, the GROMACS was used to simulate the molecular dynamics (MD) of the model. This MD analysis could provide effective theoretical method to DES design and practical approach to develop green pretreatment technology of lignocellulose biorefinery.

1. Introduction

Lignocellulosic biomass, a valuable raw material for food additives, energy products, and chemicals, has garnered global attention. In the 21st century, triggered by increasing scarcity of resources and energy, there is an urgent need to discover alternative natural resources and substitutes for fossil fuels. Agricultural and forestry waste, while contributing to environmental pressures, has garnered significant attention from researchers due to its potential as an energy source. The development of efficient, cost-effective, and environmentally friendly methods for converting biological resources into utilizable forms has become a critical research priority. Lignocellulosic biomass primarily consists of cellulose, hemicellulose, and lignin, forming a complex lignin-carbohydrate structure (Guo et al., 2021). Cellulose is composed of pyranose (C-6 sugar), while hemicellulose mostly contains furanose (C-5 sugar) monomers. As fibrous polysaccharides, They are theoretically well suited to be used as raw materials to produce carbohydrate compounds and various biofuels (Qin et al., 2023; Zhou et al., 2024). The conversion of lignocellulosic biomass into readily utilizable monosaccharides and low molecular weight compounds presents significant technical challenges. Consequently, the deconstruction of the inherent structural recalcitrance of biomass represents a critical prerequisite for efficient bioconversion processes. Numerous methods have been developed with notable success. Acid hydrolysis, which uses various acids or acidic compounds, allows for controlled temperature and time to produce XOS and facilitate the degradation of cellulose (Henriques et al., 2021). Similar to acid hydrolysis, auto hydrolysis, also known as self-hydrolysis, can result in more XOS yield and less glucan loss (Lian et al., 2020). Besides, enzymatic hydrolysis (Akpinar et al., 2007; Lv et al., 2023), steam explosion (Alvarez et al., 2020), ionic liquid pretreatment (Sun et al., 2013) and deep eutectic solvent (DES) pretreatment are also comprehensively studied. However, the limitations associated with these methods cannot be overlooked, including the high temperature requirements and equipment corrosion in acid hydrolysis, the substantial cost of ionic liquids, and the necessity for high-pressure equipment in steam explosion.

* Correspondence to: College of Chemical Engineering, Nanjing Forestry University, No. 159 Longpan Road, Nanjing 210037, PR China
E-mail address: xuyong@njfu.edu.cn (Y. Xu).

https://doi.org/10.1016/j.indcrop.2025.120805
Received 23 December 2024; Received in revised form 14 February 2025; Accepted 1 March 2025
Available online 10 March 2025

DES is a novel solvent composed of one or more hydrogen-bind donor (HBD) and one or more hydrogen-bond acceptor (HBA). As a result of this combination, the melting point of the substance in the DES system is significantly lower than that of the substances composing it, and is often liquid at room temperature (Yu et al., 2021). Since the combination of them mainly depends on hydrogen bonds, a DES system can be formed with several HBAs and HBDs, such as the common ternary deep eutectic solvent (TDES) composed of one HBA and two HBDs. The strong intramolecular hydrogen bond of these DES can break the intermolecular hydrogen bond binding in cyclic biomass (Chen and Mu, 2019; Wang et al., 2022). Thus, some DES can be suitable for the removal of lignin and hemicellulose, including choline chloride (ChCl): urea (U) (Peng et al., 2023), ChCl:lactic acid (LA) (Sai and Lee, 2019), ChCl:glycerol (GL) (Wan and Mun, 2017). Song et al. (2023) applied acid-alkane co-catalysis combined with DES pretreatment, successfully improved the biological hydrogen production efficiency of corn stover. Liu et al. (2017) used the DES system of ChCl-oxalic acid dihydrate to efficiently break the lignin-carbohydrate binding with the assistance of microblog, extracted lignin and carried out a variety of characteristics, which confirmed the application potential of DES for lignin extraction. The pretreatment effect of DES on biomass is often compared to that of ionic liquid because their mechanisms are similar (Abe et al., 2010; Huang et al., 2021). The primary advantages of DES lie in their cost-effectiveness and straightforward preparation process. These solvents demonstrate selective extraction capabilities for lignin, cellulose, and hemicellulose components (Hong et al., 2023); DES compositions exhibit non-toxic characteristics and demonstrate favorable biocompatibility (Procentese et al., 2017); its versatile application extends to feed formulations (Ma et al., 2021); and recycling is possible (Chen et al., 2023). Compared with various catalytic hydrolysis methods, the effect of DES pretreatment is more significant, the removal rate is high, and often does not require harsh reaction environment (high temperature, high pressure or acid reaction environment). As have been reported, several kinds of DES can be used as feed additives, which can avoid complex separation processes, including ChCl-LA, ChCl-U, ChCl-GL, ChCl-acetic acid, and other betaine-based DES with similar HBDs. However, excessive addition of some components (such as U and GL) may be harmful to livestock, especially in DES with a high proportion of HBD (1:5, 1:10 or higher). Therefore, reducing the amount of these components and maintaining a good pretreatment efficiency has become a promising research direction for promoting the use of DES-pretreated biomass as feed additives.

Studies on the destruction mechanism of various DES on lignocellulose architecture and lack of systematic. Most of the explanations of the mechanism are based on the speculation of experimental phenomena (Xu et al., 2020). DES can be constructed in a variety of combinations, and different ratios can also be used in one scheme. Therefore, reliable theoretical guidance is urgently needed to help researchers construct DES and improve processing efficiency and reduce cost. Both molecular dynamics (MD) (Wang et al., 2023) simulations and quantum chemical (QC) (Wu et al., 2023) calculations are methods to simulate and observe the component distributions and solvation effects in DES systems. Among them, the role of MD is analyzing the interaction between DES and cellulose, hemicellulose, lignin, including hydrogen bonding and van der Waals forces, which can help to explain the mechanism of DES on the strong hydrogen bonding network of lignocellulose; QC focuses on the weak interaction between molecules and plays an auxiliary role in MD. Density functional theory (DFT) calculation is most commonly applied in QC.

In this study, cellulose, hemicellulose, and lignin were modeled, and their interactions with TDES were investigated using MD simulations. The simulations, conducted under experimental conditions, aimed to elucidate the experimental phenomena and mechanisms of TDES-lignocellulose interactions. Key aspects such as the number of hydrogen bonds and radial distribution function (RDF) data were analyzed to reflect energy changes and interactions among the models. The study examined the impact of varying proportions of HBD and water content on treatment efficacy, offering theoretical insights for guiding subsequent experiments and predicting experimental outcomes. Post-simulation analysis highlighted the hydrogen bonding relationships between TDES and cellulose-hemicellulose, as well as cellulose-lignin, providing robust support for the MD simulation results.

2. Materials and methods

2.1. DES construction and biomass preparation

DES was prepared by mixing HBDs including GL, citric acid (CA) and HBA which was ChCl in different molar ratios. They were transferred into 250 mL conical flasks and subjected to water baths maintained at varying temperatures, accompanied by magnetic stirring for different time. Upon completion of the reaction, a homogeneous and transparent viscous liquid should be obtained. In D4-D7, different ratio (w:w) of deionized water were added to the DES system before the pretreatment was performed. Details are shown in Table 1.

Sugarcane bagasse (SB) material involved in this study was purchased from Hainan province, China. SB was air-dried and then smashed, and 40–80 meshed SB was harvested for the subsequent treatments. The main chemical components of SB were analyzed by the protocol of the National Renewable Energy Laboratory (NREL) standard method, which showed that it is mainly composed of 35.15 % glucan, 20.91 % xylan, 0.94 % acid-soluble lignin and 6.174 % acid-insoluble lignin.

2.2. Pretreatment of SB

The DES pretreatment of SB was performed in a 50 mL stainless steel tank by mixing 3 g dry SB with 30 g DES. The tank was heated at different temperatures ranging from 80 ℃ to 120 ℃ in an oil bath for 30–60 min. The whole tank was cooled down with cold water immediately after the pretreatment ended and the mixture was collected. 1:5 (w:v) ethanol was poured into the mixture in three times and vortexed to obtain a uniform slurry, and then centrifuged to separate the solid and liquid phases and collected separately. Thereafter, the resulting solid slag was washed using deionized water until the last wash did not contain Cl^- (taking the filtrate and adding silver nitrate solution by dropping did not produce precipitation). The washed material was physically extruded out of excess water and naturally air-dried to obtain wet material, which was stored in the −4 ℃ refrigerator for subsequent processing and analysis.

2.3. Enzymatic hydrolysis and analysis

The components of SB and process materials are measured following the protocol of NREL. High-performance liquid chromatography (HPLC, Agilent 1200, USA) equiped with HPX-87H column (Aminex Bio-Rad, USA) was used for simultaneously determining xylose and glucose. Xylose and XOS (including xylobiose (X2), xylotriose (X3), xylotetraose (X4), xylopentaose (X5), and xylohexaose (X6)) are determined with High-Performance Anion Exchange Chromatography (HPAEC) which pulsed amperometric detection and a CarboPac™ PA200 column.

Both raw SB materials along with all treated SB are submitted to an enzymatic hydrolysis experiment to gain glucose, where raw SB acts as a control group. In the enzymatic hydrolysis experiment, the whole system contained 0.25 g of dry material (calculated by water content), the environment was 0.1 M sodium citrate buffer, cellulase concentration of 20 FPIU/g glucan (Cellic CTec2, Novozymes, NA, Franklinton, USA), and the total liquid volume was 20 mL. The mixture was loaded in 100 mL volume screw capped bottles and sealed, and the reaction was carried out in a shaking water bath at 50 ℃ for 72 h. Upon completion of the hydrolysis process, the reaction vessels were immediately immersed in ice-cold water to terminate the reaction. Samples were collected at

Table 1
Construction details of 7 DES systems.

DES	Component	HBA	HBD	HBD 2	Molar Ratio	Time	Temperature	Water addition
D1	ChCl:CA	ChCl	CA	/	1:2	3 h	100℃	/
D2	ChCl:GL	ChCl	GL	/	1:2	2 h	80℃	/
D3	ChCl:GL:CA	ChCl	GL	CA	1:1:1	2 h	80℃	/
D4	ChCl:GL:CA	ChCl	GL	CA	1:1:1	2 h	80℃	5 % water added
D5	ChCl:GL:CA	ChCl	GL	CA	1:1:1	2 h	80℃	20 % water added
D6	ChCl:GL:CA	ChCl	GL	CA	1:1:1	2 h	80℃	50 % water added
D7	ChCl:GL:CA	ChCl	GL	CA	1:1:1	2 h	80℃	100 % water added

30 min, 60 min, 120 min, and 240 min intervals for subsequent analysis to determine the enzymatic hydrolysis efficiency, which was calculated using the following formula:

$$\text{Efficiency}(\%) = \frac{m_{g1} + m_{c1}}{m_{g2}} \times 100\%$$

In the formula, m_{g1} represents the glucose concentration in the hydrolysate, while m_{c1} represents the cellobiose concentration in the hydrolysate; m_{g2} corresponds to the glucose in the residue obtained in DES pretreatment, as quantified by HPLC. All experiments were performed in three parallel experiments, and the experimental data presented in the paper are the average of the parallel data.

2.4. Molecular dynamics simulation

All model molecular structures were optimized to a minimum energy structure using Gaussian 09 W software at the B3LYP-D3 (BJ)/def2-SVP level. Optimized structures are shown in Fig. 1. Thereafter, the data were submitted for single-point energy calculation at the B3LYP-D3 (BJ)/def2-TZVP level to obtain molecular wave function information. It has been reported that the RESP charge is the most suitable atomic charge for MD simulation of flexible small molecules, so this paper uses the RESP charge to calculate the charges of all atoms. The Multiwfn version 3.3.6 program (Lu and Chen, 2012) was used to calculate the RESP charges of all molecules based on the surface electrostatic potential information. The optimized molecules were obtained from the CHARMM36 force field molecular topology file which is downloaded from the CGenFF website.

MD simulations were all conducted using GROMACS 2020.3_GPU (Pronk et al., 2013). The force field file used in the simulation was the Charmm36 force field under which all molecules are parameterized. A total of 6 systems were constructed and the detailed information are as follows:

System 0: 12 hemicellulose, 12 cellulose and 12 lignin molecules were mixed for 50 ns kinetic simulations. Temperature: 100 ℃; Pressure: 1 bar.

System 1: 200 ChCl: 200 GL: 200 CA was mixed with 12 hemicellulose, 12 cellulose and 12 lignin molecules for 50 ns kinetic simulations. Temperature: 100 ℃; Pressure: 1 bar.

System 2: 200 ChCl: 400 GL was mixed with 12 hemicellulose,12 cellulose of and 12 lignin molecules for 50 ns kinetic simulations. Temperature: 100 ℃; Pressure: 1 bar.

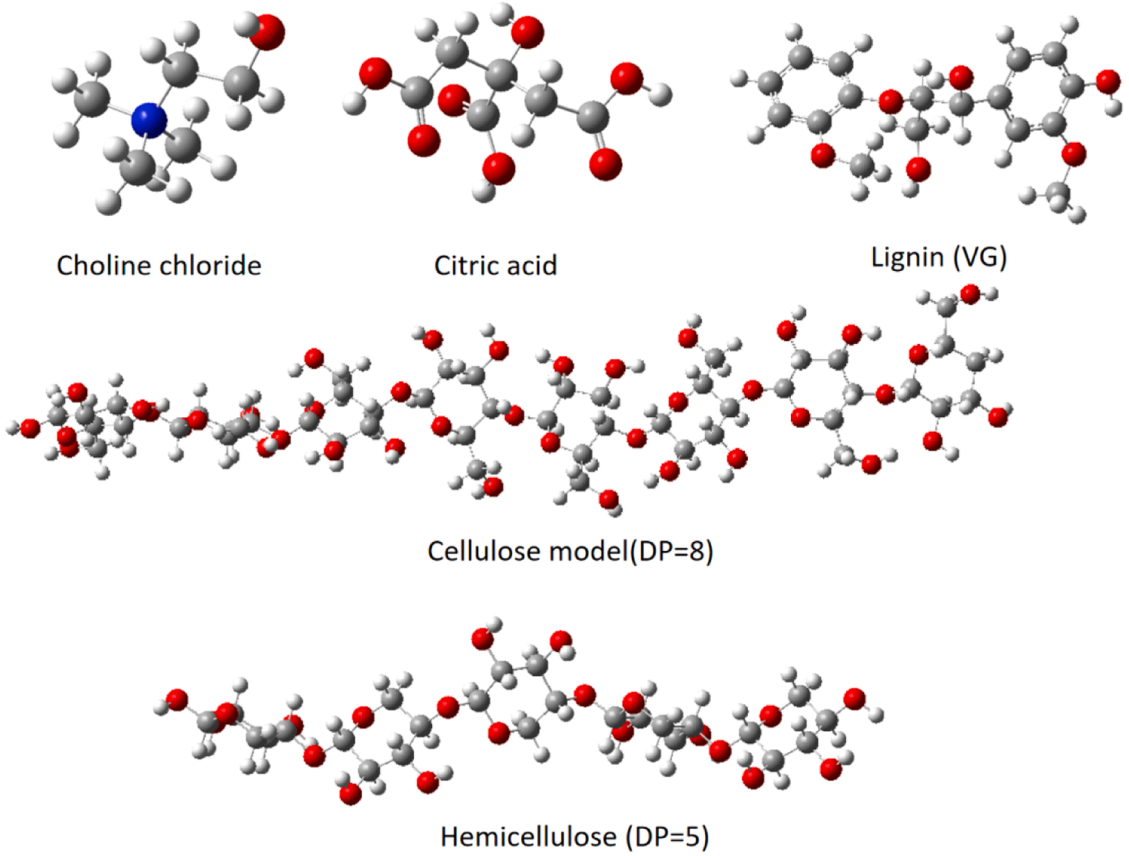

Fig. 1. Optimized structure of choline chloride, ctric acid, lignin (VG model), cellulose model and hemicellulose model.

System 3: 200 ChCl: 400 CA was mixed with 12 hemicellulose, 12 cellulose and 12 lignin molecules for 50 ns kinetic simulations. Temperature: 100 ℃; Pressure: 1 bar.

The system 4: 1:1:1 molar ratio of 200 ChCl: 200 GL: 200 CA was mixed with 12 hemicellulose, 12 cellulose 12 lignin molecules, and 20 % of the total mass of water molecules was added for 50 ns kinetic simulation. Temperature: 100 ℃; Pressure: 1 bar.

The system 5: 1:1:1 molar ratio of 200 ChCl: 200 GL: 200 CA was mixed with 12 hemicellulose, 12 cellulose and 12 lignin molecules, then 50 % of the total mass of water molecules was added for 50 ns kinetic simulation. Temperature: 100 ℃; Pressure: 1 bar.

The steepest descent method was used to minimize the energy of the system at 298.15 K and 1 bar pressure. A total of 50,000 simulation steps were performed. All the system temperatures in this simulation are 373.15 K. After reaching this temperature, the energy minimization system is simulated in the NVT system for 100 ps and then in the NPT system for 50 ps to obtain the limiting dynamics of the simulated system. Finally, the system was submitted to long-range calculations at 373.15 K with a pressure of 1 bar for 50 ns (25,000,000 steps). After the system was established, based on the data above and the simulated trajectory literature, the hydrogen bond count, intermolecular force and radial distribution function (RDF) data in the system were paid attention to and obtained for the result analysis.

3. Results and discussion

3.1. DES pretreatment effect of SB

SB was mixed with D1 to D3 and reacted at 80 °C, 100 °C, and 120 °C for 30 min, 60 min, 120 min, and 240 min to identify optimal pretreatment conditions. The composition of the solid fractions isolated after treatment and their enzymatic pretreatment efficiency are presented in Fig. 2. The results indicate that increasing the reaction temperature slightly improves the removal rate of hemicellulose and lignin for the same DES system. However, higher reaction temperatures (120 °C) actually reduce the efficiency of subsequent enzymatic hydrolysis. This may be due to the effect of high temperature on the lignin component or the reinforcement of the crystalline zone (Yao et al., 2024). The enzymatic hydrolysis kinetic curves of the samples are shown in Fig. 3.

For the pretreatment using D1, increasing time and temperature had a limited impact on enhancing the pretreatment effectiveness. The exposure of cellulose components was similar to that of the raw biomass, resulting in unsatisfactory enzymatic hydrolysis. The best enzymatic hydrolysis effect achieved was 42.57 % at 120 °C for 240 min. This is normal according to the general scientific understanding, because the application of CA-formed DES in pretreatment is not satisfactory, unless coupled with other auxiliary means, such as microwaves(Liu et al., 2021; Wang et al., 2024; Yadav et al., 2024). GL is the primary HBD in D2, and previous studies have demonstrated its efficacy in exposing cellulose in biomass, which aligns with the findings of this study(Jiang et al., 2024). After treatment with D2, the proportion of cellulose in the solid residue increased while the lignin proportion decreased, leading to improved enzymatic hydrolysis. The optimal conditions for D2 were 100 °C for 240 min, resulting in an enzymatic hydrolysis effect of 53.93 %. This is also consistent with previous research papers (Li et al., 2024). D3, which combines two HBDs in a 1:1:1 molar ratio, maintains the same overall HBD to HBA ratio as D1 and D2. Pretreatment with D3 yielded a more satisfactory enzymatic hydrolysis effect. At 80 °C, more xylans were dissolved compared to pretreatment with D1 and D2 at the

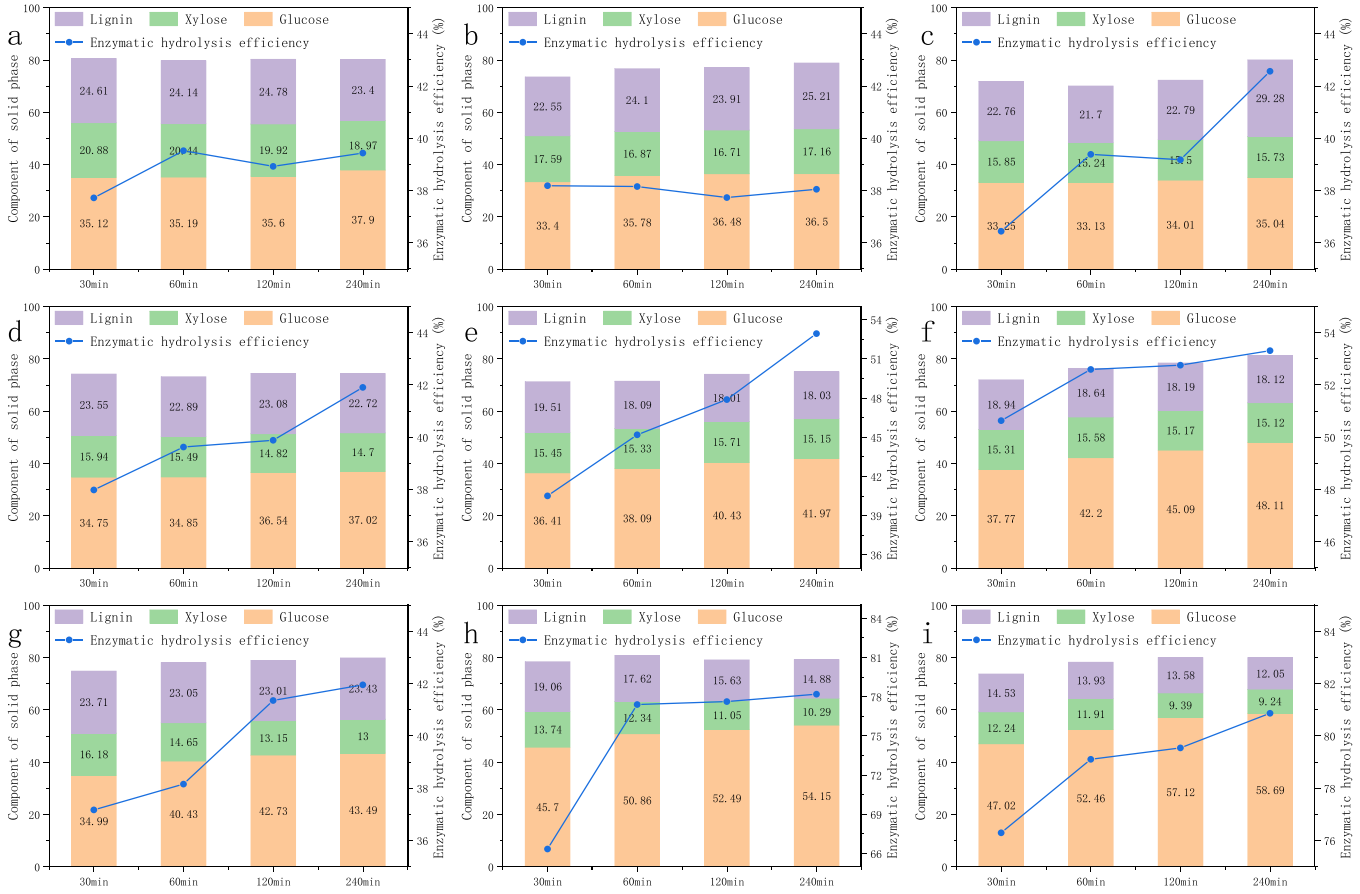

Fig. 2. Composition of the solid fractions isolated after treatment and their enzymatic pretreatment efficiency. (a) 80 ℃, D1. (b) 100 ℃, D1. (c) 120 ℃, D1. (d) 80 ℃, D2. (e) 100 ℃, D2. (f) 120 ℃, D2. (g) 80 ℃, D3. (h) 100 ℃, D3. (i) 120 ℃, D3.

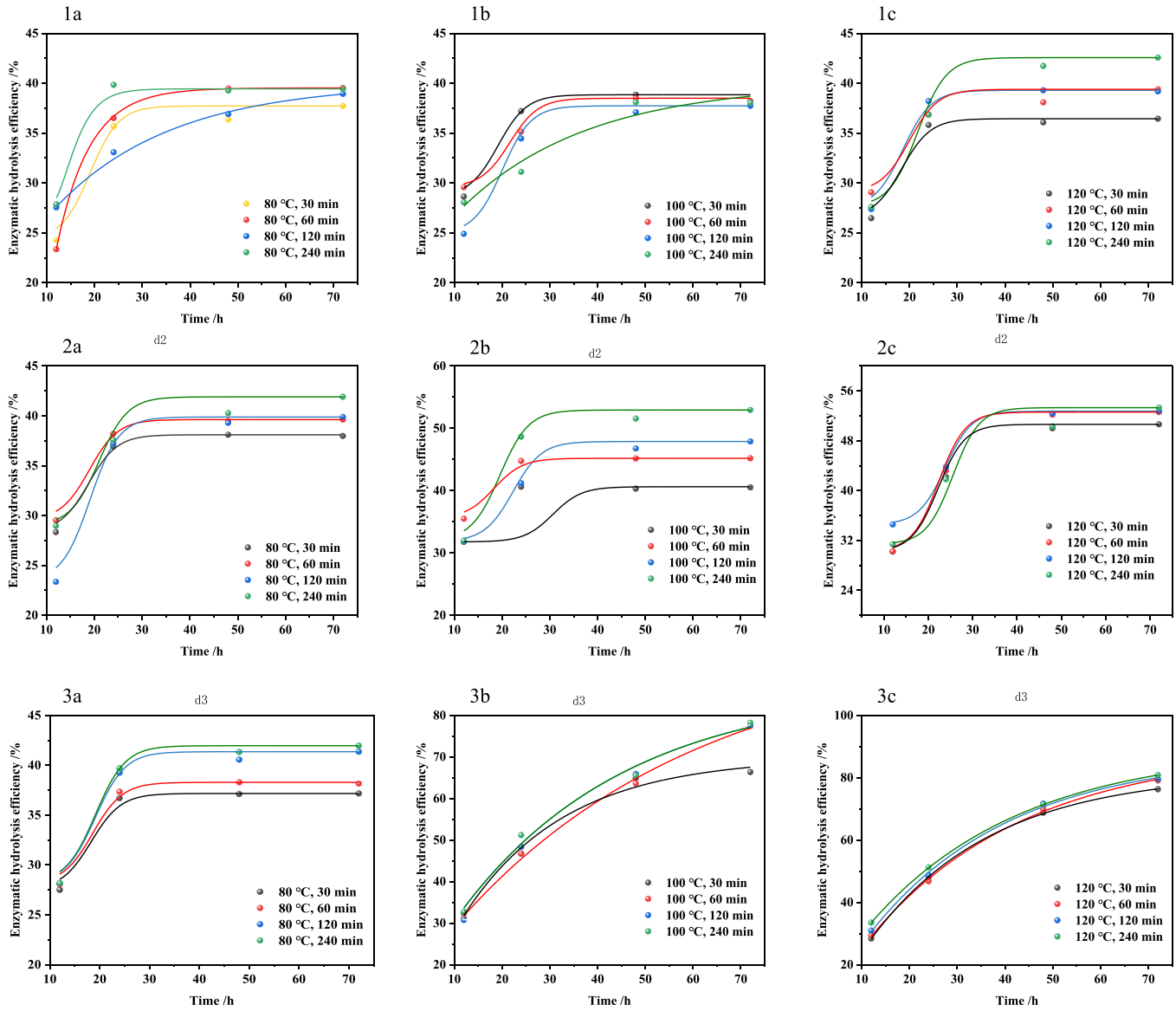

Fig. 3. Enzymatic hydrolysis kinetic curves. (1a,1b,1c) Pretreated by D1. (2a,2b,2c) Pretreated by D2. (3a,3b,3c) Pretreated by D3.

same temperature, leading to an increased cellulose content in the solid residue. However, the enzymatic hydrolysis effect after 240 min of treatment was only 41.96 %, slightly higher than that of D2 (41.91 %). This phenomenon may be attributed to insufficient temperature to disrupt the weak intermolecular interactions, consequently leading to the dissolution of loosely bound xylan without contributing to the enhancement of enzymatic hydrolysis efficiency. At 100 °C, pretreatment effectiveness improved significantly. After 30 min, the cellulose content in the solid residue reached 45.7 %, and the enzymatic hydrolysis efficiency increased to 66.35 %. After 60 min, the cellulose content rose to 50.86 %, with enzymatic hydrolysis efficiency reaching 77.4 %. Longer treatment times did not significantly enhance cellulose exposure or enzymatic hydrolysis efficiency; even after 240 min, the efficiency only increased to 78.20 %. A similar pattern was observed at 120 °C. Although enzymatic hydrolysis efficiency improved with increased temperature, the maximum efficiency was only 80.87 % at 120 °C for 240 min. Given that 100 °C is more practical for actual operations, we recommend 100 °C and 60 min as the optimal treatment conditions. This condition will serve as the baseline for further experimental and theoretical studies.

3.2. *Effect of the presence of water in TDES on pretreatment*

D4-D7 compared the effect of different water contents on the pretreatment effect of TDES system. The result of enzymatic hydrolysis is shown in Table 2.

In all groups, the addition of water consistently enhanced the enzymatic hydrolysis of TDES-treated solid residues. With 20 % water content, the enzymatic hydrolysis efficiency reached 92.84 %. Further increases in water content did not yield additional improvements in pretreatment effectiveness. This is consistent with previous literature (Li et al., 2022; Xu et al., 2023). This phenomenon may result from a combination of factors. Firstly, the high viscosity of most DES systems leads to inefficient mass transfer, preventing adequate contact between DES and biomass (Zhang et al., 2024). Adding water reduces the

Table 2
Enzymatic hydrolysis result of D3-D7 (100℃, 60 min).

DES	D3	D4	D5	D6	D7
Enzymatic hydrolysis efficiency	77.40 %	92.84 %	92.93 %	83.63 %	85.60 %

system's viscosity, thereby enhancing mass transfer. Additionally, water can form strong hydrogen bonds, which may disrupt the original hydrogen bond network of the DES, creating a more complex network that more effectively breaks hydrogen bonds in the biomass, thus improving pretreatment. However, excessive water can dilute the DES and potentially cause some HBD and HBA to dissociate into free ions, diminishing the advantages of DES pretreatment. To test these hypotheses, we employed MD simulations.

3.3. Interpretation and analysis with MD simulations

In order to investigate the effect of DES on lignocellulose, various MD simulation results are analyzed in this section, trying to explain the experimental phenomena observed. As a control group, three models without DES (including VG model representing lignin, cellulose and hemicellulose) were first analyzed to simulate the structure of native lignocellulose. The number of hydrogen bonds can systematically and intuitively show the interaction between DES and lignocellulose system. Fig. 4**a**. shows the influence of the addition of different DES on the number of hydrogen bonds among the three components of lignocellulose. Observing the untreated control group, it was found that the number of hydrogen bonds between cellulose and hemicellulose was the largest, accounting for 65.04 % of the total number of hydrogen bonds, followed by the number of hydrogen bonds between hemicellulose-lignin. This is because the well-known network of hydrogen bonds formed between the -OH groups of polysaccharides, one of the key factors that prevents the enzyme from accessing the cellulolytic site. The reason why hemicellulose binds more closely to lignin than cellulose may be that cellulose is more rigid and lignin has difficulty accessing more -OH groups to form enough hydrogen bonds.

The addition of DES significantly reduced the number of hydrogen bonds in the three components and formed new hydrogen bond networks, which was consistent with previous reports. Lignin inhibits enzymatic hydrolysis mainly through electrostatic interaction and hydrophobic interaction. Hydrogen bonds formed by DES can not only loosen the LCC structure, but also reduce the overall hydrophobicity of lignocellulose. It can be seen in Fig. 4**b** that in terms of the hydrogen bond count of cellulose-hemicellulose, DES1 has a better effect on reducing the number of hydrogen bonds, reducing hydrogen bonds by 82.52 %. In DES4 and DES5, the addition of water has no significant effect on the treatment effect, while the 50 % water content makes the treatment effect worse, only reducing hydrogen bonds by 77.08 %. However, for the hydrogen bond count of hemicellulose-lignin, except DES2 treatment was not effective, which reduced only 84.25 % of hydrogen bonds, while the treatment effect of the other four groups of DES was similar, with reducing hydrogen bonds ranging from 91.22 % to 91.86 %. Based on Fig. 1b, from the hydrogen bonds data produced by DES and different components in each system, DES without water is more inclined to form hydrogen bonds with lignin, while DES with water and hemicellulose form hydrogen bonds slightly increased. This is probably due to the hydrophobic nature of lignin itself, which makes it difficult for the aqueous DES to access lignin molecules. By comparison with the above experimental phenomena, it can be found that pretreatment assisted with DES which is easier to form hydrogen bonds with hemicellulose is more conducive to enzymatic hydrolysis. To summarize, in lignocellulosic biomass, cellulose-cellulose and cellulose-hemicellulose are predominantly interconnected through an extensive network of hydrogen bonds within their chain-like structures. Upon interaction with these structural components, the HBD present in the DES displaces the native hydrogen bonding interactions, subsequently establishing alternative hydrogen bond networks. This molecular rearrangement results in the destabilization of the cellulose-hemicellulose matrix, thereby enhancing enzymatic accessibility. Furthermore, the newly established hydrogen bonds impart increased hydrophilicity to the structural framework, which may contribute to the observed enhancement in enzymatic hydrolysis efficiency. Fig. 5 illustrates the mechanism of DES disruption of native hydrogen bonding and the formation of a reconfigured hydrogen bond network involving cellulose, hemicellulose, and HBD components.

The interaction energy data gained in the simulation are shown in Table 3. It can be seen that no matter what kind of DES is added, the energy of electrostatic interactions and van der Waals forces are much weaker than those of system0 without DES. Among them, the interaction energy between hemicellulose and lignin itself is significantly smaller than the interaction energy between cellulose and hemicellulose, cellulose and lignin, and the addition of DES has the least significant effect on it. Taking DES as an example, Only 473.535 KJ/mol of electrostatic interaction energy and 439.158 KJ/mol of van der Waals force energy are reduced. In contrast, the interaction energy received by cellulose is significantly affected by DES. This may explain why the dissolution of lignin by DES is not complete but can improve the enzyme hydrolysis efficiency of cellulose. By comparing the total interaction energy, it can be found that for the interaction energy between cellulose and hemicellulose, DES1 treatment was the best which reduced the totel interaction energy by 4872.018 KJ/mol, followed by DES4 treatment which reduced by 4814.066 KJ/mol; for hemicellulose-lignin, DES4 had the best treatment effect which reduced the totel interaction energy by 1074.065 KJ/mol, followed by DES2 which is slightly weaker than that; for cellulose-lignin, DES3, DES4, and DES5 treatments all showed similarly good effects reducing the interaction energy by 2701.5376 KJ/mol, 2697.612 KJ/mol and 2667.511 KJ/mol.

The average value of the radial distribution functions (RDF) data are shown in Fig. 6. Since the role of Cl^- in DES is relatively dominant, it was chosen as the counted atom. H-bond on oxygen atoms in other different substances are defined separately, and they are clearly shown in Fig. 7. In hemicellulose, OA1 represents the ether bond connecting the two xylose molecules, and OA2-OA6 represents the hydroxyl group in xylose. In cellulose, OB1 represents the oxygen atom in the glycosidic bond and OB2-OB5 represents the hydroxyl group on glucose, both of which have the potential to form hydrogen bonds. In the lignin model, each oxygen atom that may form a hydrogen bond is defined separately, and they are designated OC1-OC6. RDF analysis shows that only in

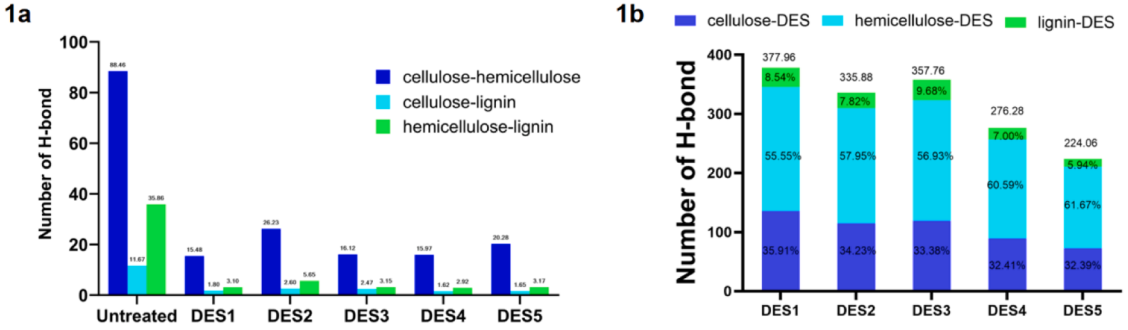

Fig. 4. Number of hydrogen bonds between DES, cellulose, hemicellulose, and lignin in each system.

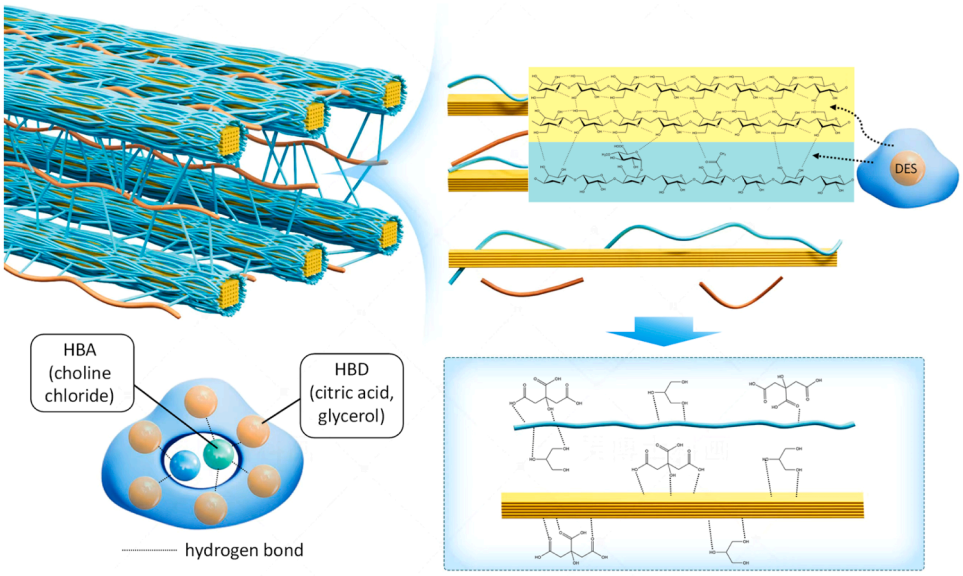

Fig. 5. Stimulated picture of the interaction between DES and lignocellulose.

Table 3
Interaction energy between lignocellulose components in each DES system.

	system0	DES1	DES2	DES3	DES4	DES5
C-HC-coul	−3651.27	−491.114	−816.871	−576.654	−589.542	−805.191
HC-LG-coul	−559.494	−85.9598	−94.4932	−58.2639	−70.8332	−81.8874
C-LG-coul	−1625.76	−112.938	−190.935	−96.3794	−129.786	−152.992
C-HC-lj	−2205.34	−493.478	−558.325	−571.72	−453.002	−692.556
HC-LG-lj	−687.798	−248.64	−84.9245	−136.922	−102.394	−134.712
C-LG-lj	−1391.94	−302.452	−258.861	−219.783	−190.302	−197.197
C-HC-total	−5856.61	−984.592	−1375.196	−1148.374	−1042.544	−1497.747
HC-LG-total	−1247.292	−334.5998	−179.4177	−195.1859	−173.2272	−216.5994
C-LG-lj-total	−3017.7	−415.39	−449.796	−316.1624	−320.088	−350.189

DES1, the highest RDF peak appears at OA3, in DES2-DES5, the highest RDF peak appears at OA5 regardless of the type of DES system, distributed at 0.314–0.326 nm around hemicellulose. Cl^- (representing DES molecule) has the highest distribution density near the carboxyl group of the xylose unit of hemicellulose. At the same time, it can be intuitively seen that the RDF peak of OA group is significantly higher than that of OB and OC groups, indicating that the hydrogen bonds between DES and hemicellulose is the strongest. In DES1, the highest RDF peak appeared at OA3-Cl, with a peak value of 7.378. In all the remaining four DES systems, the maximum peak appeared at OA5-Cl, and the peaks from DES2 to DES5 were 6.431, 7.941, 2.666, and 1.795, respectively. Based on the experimental results, this may be because a more single hydrogen bond site is more conducive to binding, or it may be because the binding at OA3 is the key to the dissolution of hemicellulose, but this conclusion needs more experiments and data to support. Meanwhile, the peak RDF at OA3-Cl in DES2 and DES3 could reach 4.782 and 5.911, respectively. Instead of clustering around xylan, these DES appear to form a complex network of hydrogen bonds. The H-bond network was drastically disrupted by the addition of water, and the RDF peaks in DES4 and DES5 became more average and decreased in peak value. Since water itself can also provide a strong hydrogen bond network, the addition of water may lead to the formation of a more complex and strong hydrogen bond network in the DES system, which can better interact with hemicellulose (and lignin).

Both experimental and molecular dynamic simulation results reflected that the newly constructed DES has an outstanding capability of deconstruct LCC and improve the enzymatic hydrolysis efficiency. This may reveal that other grass-like agricultural residue can also be pretreated through this method. For instance, corncob, corn stalk, wheat straw and other agricultural residues which possess hemicellulose fraction with mainly arabino-xylan.

4. Conclusion

Theoretical analysis and MD simulations elucidate the experimental observation that the formulated TDES exhibits superior pretreatment efficacy for SB compared to its binary DES counterpart, with the incorporation of water further enhancing specific aspects of the pretreatment process. Specifically, the presence of multiple HBDs in the ternary DES facilitates the formation of a more extensive and intricate hydrogen bonding network. This optimized network demonstrates enhanced efficiency in deconstructing the intermolecular bonds within the biomass complex and form hydrogen bonds between xylan and HBDs, thereby significantly improving pretreatment efficiency. In conclusion, this study identifies a highly effective DES formulation for biomass pretreatment. The addition of water to the optimized DES system resulted in pretreated sugarcane bagasse achieving an enzymatic hydrolysis efficiency of 92.93 %. Furthermore, the insights derived from MD simulations provide a robust theoretical framework for the future development and identification of more effective DES combinations for biomass processing applications.

Abbreviations Used
(CA) citric acid
(ChCl) choline chloride
(DES) deep eutectic solvent
(GL) glycerol
(HBA) hydrogen-bond acceptor
(HBD) hydrogen-bind donor

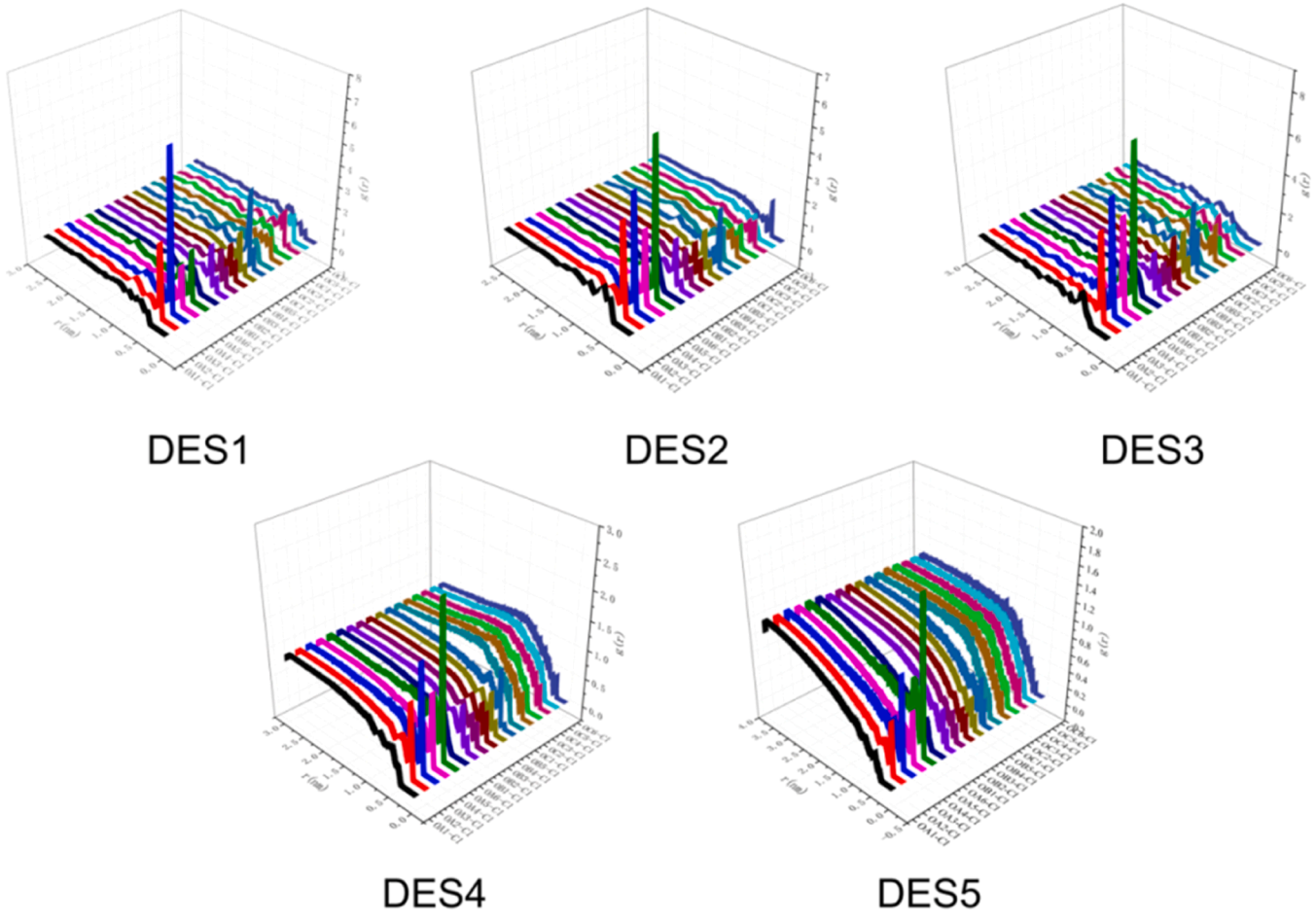

Fig. 6. RDF data of DES1 to DES 5.

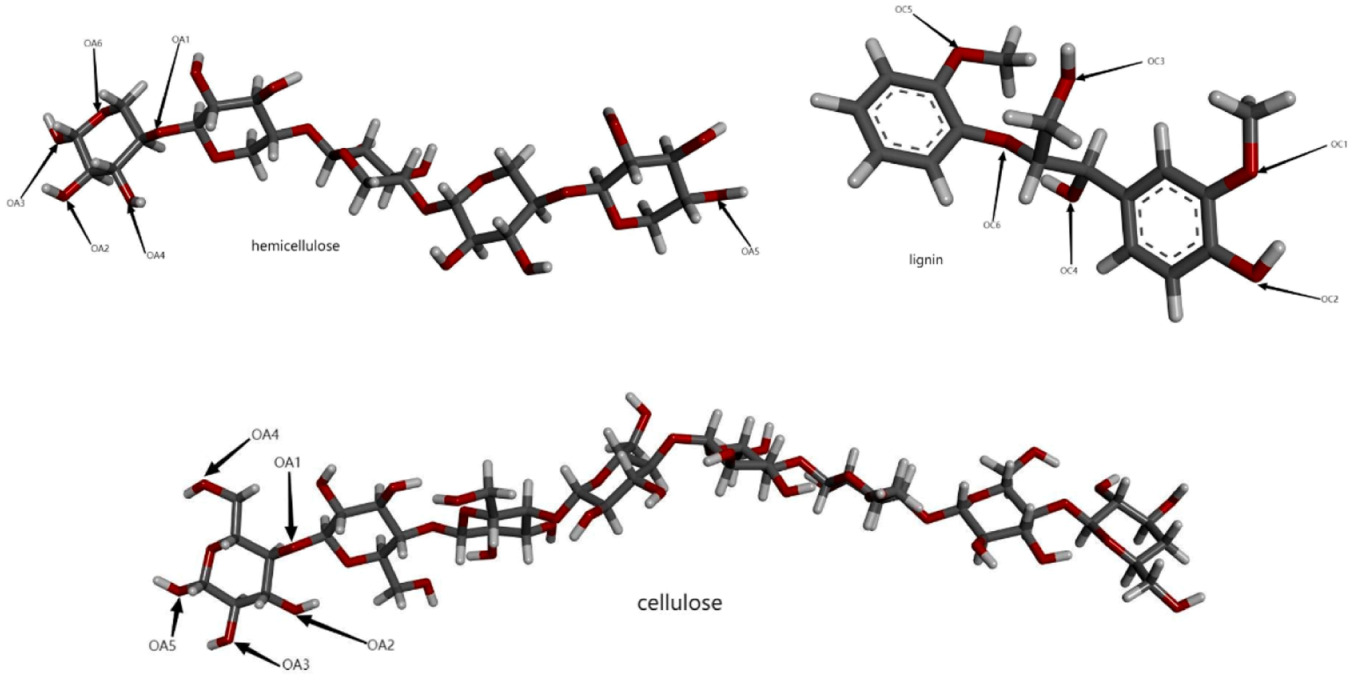

Fig. 7. Define the numbering of oxygen atoms in the cellulose, hemicellulose, lignin models.

(MD) molecular dynamics
(RDF) radial distribution function
(SB) sugarcane bagasse (SB)
(TDES) ternary deep eutectic solvent

Ethics approval and consent to participate

Not applicable

Consent for publication

Not applicable.

Author's contributions

SZ and YX designed the project, and SZ looked for papers, read and categorized them, carried out experiments then finished manuscript writing. YX and XZ helped to revise the manuscript. YX supervised the project. All authors read and approve the final manuscript.

Ethics approval and consent to participate

Not applicable

Consent for publication

Not applicable.

Funding

This work was supported by the National Key R&D Program of China (2022YFD1300903), and the National Natural Science Foundation of China (32171730, 32211530071).

CRediT authorship contribution statement

Xu Yong: Writing – review & editing, Validation, Supervision, Funding acquisition. **Zhou Shaonuo:** Software, Methodology, Investigation, Formal analysis, Data curation, Conceptualization. **Zhang Xiaolei:** Supervision, Resources, Investigation.

Declaration of Competing Interest

There are no conflicts to declare.

Data availability

The data that has been used is confidential.

References

Abe, M., Fukaya, Y., Ohno, H., 2010. Extraction of polysaccharides from bran with phosphonate or phosphinate-derived ionic liquids under short mixing time and low temperature. Green Chem. 12 (7), 1274–1280.
Akpinar, O., Ak, O., Kavas, A., Bakir, U., Yilmaz, L., 2007. Enzymatic production of xylooligosaccharides from cotton stalks. J. Agric. Food Chem. 55 (14), 5544–5551.
Alvarez, C., Gonzalez, A., Alonso, J.L., Saez, F., Negro, M.J., Gullon, B., 2020. Xylooligosaccharides from steam-exploded barley straw: structural features and assessment of bifidogenic properties. Food Bioprod. Process. 124, 131–142.
Chen, T., Guo, G., Shen, D., Tang, Y., 2023. Metal salt-based deep eutectic solvent pretreatment of moso bamboo to improve enzymatic hydrolysis. Fermentation 9 (7).
Chen, Y., Mu, T., 2019. Application of deep eutectic solvents in biomass pretreatment and conversion. Green Energy Environ. 4 (2), 95–115.
Guo, J., Gu, Y., Zhou, X., Xu, B., Wang, H., Xu, Y., 2021. Cascade temperature-arising strategy for xylo-oligosaccharide production from lignocellulosic biomass with acetic acid catalyst recycling operation. Renew. Energy 175, 625–637.
Henriques, P., Martinho, M., Serrano, Md.L., Mendes de Sousa, A.P., Brites Alves, A.M., 2021. Xylooligosaccharides production by acid hydrolysis of an alkaline extraction filtrate from Eucalyptus globulus bleached kraft pulp. Ind. Crops Prod. 159.
Hong, S., Wang, P.F., Xiao, M.Z., Shen, X.J., Liu, J., Cao, X.F., Yuan, T.Q., Products. 2023. Facile and sustainable preparation of hierarchical porous carbon material from lignin/DES mixture after pretreatment. 193, 116211-.
Huang, K., Mohan, M., George, A., Simmons, B.A., Xu, Y., Gladden, J.M., 2021. Integration of acetic acid catalysis with one-pot protic ionic liquid configuration to achieve high-efficient biorefinery of poplar biomass. Green Chem. 23 (16), 6036–6049.
Jiang, H., Lou, L., Nie, J., Zhang, A., Ge, L., Xie, J., Chen, Y., 2024. Efficient conversion of corn stover to glucose using alkaline DBU synergized glycerol-based deep eutectic solvent under mild conditions. Ind. Crops Prod. 222.
Li, W., Ma, S., Luo, L., Li, Z., He, A., Wang, C., Lin, L., Zeng, X., 2024. Pretreatment of biomass with ethanol/deep eutectic solvent towards higher component recovery and obtaining lignin with high β-O-4 content. Int. J. Biol. Macromol. 276.
Li, N., Meng, F., Yang, H., Shi, Z., Zhao, P., Yang, J., 2022. Enhancing enzymatic digestibility of bamboo residues using a three-constituent deep eutectic solvent pretreatment. Bioresour. Technol. 346.
Lian, Z., Wang, Y., Luo, J., Lai, C., Yong, Q., Yu, S., 2020. An integrated process to produce prebiotic xylooligosaccharides by autohydrolysis, nanofiltration and endo-xylanase from alkali-extracted xylan. Bioresour. Technol. 314.
Liu, Y., Chen, W., Xia, Q., Guo, B., Wang, Q., Liu, S., Liu, Y., Li, J., Yu, H., 2017. Efficient cleavage of lignin-carbohydrate complexes and ultrafast extraction of lignin oligomers from wood biomass by microwave-assisted treatment with deep eutectic solvent. ChemSusChem 10 (8), 1692–1700.
Liu, W., Du, H., Liu, K., Liu, H., Xie, H., Si, C., Pang, B., Zhang, X., 2021. Sustainable preparation of cellulose nanofibrils via choline chloride-citric acid deep eutectic solvent pretreatment combined with high-pressure homogenization. Carbohydr. Polym. 267.
Lu, T., Chen, F., 2012. Multiwfn: a multifunctional wavefunction analyzer. J. Comput. Chem. 33 (5), 580–592.
Lv, D., Zhang, W., Meng, X., Liu, W., 2023. Single mutation in transcriptional activator Xyr1 enhances cellulase and xylanase production in trichoderma reesei on glucose. J. Agric. Food Chem. 71 (31), 11993–12003.
Ma, C.-Y., Xu, L.-H., Zhang, C., Guo, K.-N., Yuan, T.-Q., Wen, J.-L., 2021. A synergistic hydrothermal-deep eutectic solvent (DES) pretreatment for rapid fractionation and targeted valorization of hemicelluloses and cellulose from poplar wood. Bioresour. Technol. 341.
Peng, J., Xu, Y., Zhu, B., Yu, H., Li, B., Xu, H., 2023. Life cycle assessment of bioethanol production by two methods of pretreatment of rice straw based on process simulation. Ind. Crops Prod. 191.
Procentese, A., Raganati, F., Olivieri, G., Russo, M.E., Rehmann, L., Marzocchella, A., 2017. Low-energy biomass pretreatment with deep eutectic solvents for bio-butanol production. Bioresour. Technol. 243, 464–473.
Pronk, S., Pall, S., Schulz, R., Larsson, P., Bjelkmar, P., Apostolov, R., Shirts, M.R., Smith, J.C., Kasson, P.M., van der Spoel, D., Hess, B., Lindahl, E., 2013. GROMACS 4.5: a high-throughput and highly parallel open source molecular simulation toolkit. Bioinformatics 29 (7), 845–854.
Qin, R.-C., Ma, Y.-Y., Wang, D., Bao, N.-Z., Liu, C.-G., 2023. Preparation of cellulose nanofibers from corn stalks by fenton reaction: a new insight into the mechanism by an experimental and theoretical study. J. Agric. Food Chem.
Sai, Y.W., Lee, K.M., 2019. Enhanced cellulase accessibility using acid-based deep eutectic solvent in pretreatment of empty fruit bunches. Cellulose 26 (18), 9517–9528.
Song, W., Jiang, J., Jiang, H., Liu, C., Dong, Y., Chen, X., Xiao, L.-P., 2023. Acid/alkali-catalyzed deep eutectic solvent pretreatment of corn straw for enhanced biohydrogen production. Fuel 348.
Sun, S.-N., Li, M.-F., Yuan, T.-Q., Xu, F., Sun, R.-C., 2013. Effect of ionic liquid/organic solvent pretreatment on the enzymatic hydrolysis of corncob for bioethanol production. Part 1: Structural characterization of the lignins. Ind. Crops Prod. 43, 570–577.
Wan, Y.L., Mun, Y.J. 2017. Assessment of natural deep eutectic solvent pretreatment on sugar production from lignocellulosic biomass. In: Proceedings of the 9th International Engineering Research Conference (Eureca), 2018 Dec 06, Taylors Univ, Subang Jaya, MALAYSIA.
Wang, W., Kong, Y., Peng, J., Li, B., Xu, H., 2022. Probing the mechanism of green solvent solubilization of hemicellulose based on molecular dynamics simulations. Ind. Crops Prod. **186**.
Wang, N., Xu, A., Liu, K., Zhao, Z., Li, H., Gao, X., 2024. Performance of green solvents in microwave-assisted pretreatment of lignocellulose. Chem. Eng. J. 482.
Wang, W., Xu, Y., Zhu, B., Ge, H., Wang, S., Li, B., Xu, H., 2023. Exploration of the interaction mechanism of lignocellulosic hybrid systems based on deep eutectic solvents. Bioresour. Technol. 385.
Wu, X., Yuan, Y., Hong, S., Xiao, J., Li, X., Lian, H., 2023. Controllable preparation of nano-cellulose via natural deep eutectic solvents prepared with lactate and choline chloride. Ind. Crops Prod. **194**.
Xu, H., Kong, Y., Peng, J., Song, X., Che, X., Liu, S., Tian, W., 2020. Multivariate analysis of the process of deep eutectic solvent pretreatment of lignocellulosic biomass. Ind. Crops Prod. **150**.
Xu, Y., Ma, C.-Y., Sun, S.-C., Zhang, C., Wen, J.-L., Yuan, T.-Q., 2023. Fractionation and evaluation of light-colored lignin extracted from bamboo shoot shells using hydrated deep eutectic solvents. Bioresour. Technol. 387.
Yadav, A., Sharma, V., Tsai, M.-L., Sharma, D., Nargotra, P., Chen, C.-W., Sun, P.P., Dong, C.-D., 2024. Synergistic microwave and acidic deep eutectic solvent-based pretreatment of Theobroma cacao pod husk biomass for xylooligosaccharides production. Bioresour. Technol. 400.
Yao, Z., Chong, G., Guo, H., 2024. Deep eutectic solvent pretreatment and green separation of lignocellulose. Appl. Sci. 14 (17).

Yu, D., Xue, Z., Mu, T., 2021. Eutectics: formation, properties, and applications (vol 50, pg 8596, 2021). Chem. Soc. Rev. 50 (16).
Zhang, L., Zhang, C., Ma, Y., Zhao, X., Zhang, X., 2024. Lignocellulose pretreatment by Deep eutectic solvent and water binary system for enhancement of lignin extraction and cellulose saccharification. Ind. Crops Prod. 211.
Zhou, L., Zhang, Y., Chen, T., Yun, J., Zhao, M., Zabed, H.M., Zhang, C., Qi, X., 2024. Metabolic remodulation of chassis and corn stover bioprocessing to unlock 3-hydroxypropionic acid biosynthesis from agrowaste-derived substrates. J. Agric. Food Chem. 72 (5), 2536–2546.